Paper presented at the 6th International Conference on Radiation Shielding (6th ICRS), May 16-20, 1983, Tokyo, Japan. To be published in proceedings of the conference.

U.S. INTOR RADIATION SHIELD DESIGN*

Y. Gohar and M. A. Abdou **

Fusion Power Program
Argonne National Laboratory
9700 South Cass Avenue
Argonne, IL 60439

May, 1983

* Work supported by the U.S. Department of Energy.

** Now located at University of California, Los Angeles.

U.S. INTOR RADIATION SHIELD DESIGN*

Y. Gohar and M. A. Abdou
Argonne National Laboratory
Argonne, Illinois, USA

ABSTRACT

The U.S. analysis for the INTOR radiation shield design focused on three areas. First, a careful optimization process for the inboard shield composition and material arrangement within the allowable radial shield thickness was performed to minimize the radiation effects in the toroidal field (TF) coils. The TF coils are designed to last the lifetime of the reactor without change in performance. Second, the outboard bulk shield composition and material arrangement were optimized to achieve a dose equivalent outside the bulk shield of ≤ 2.5 mrem/h within one day after shutdown to permit personnel access to the reactor hall. Third, the penetration shields were designed to satisfy the same requirements as the outboard bulk shield.

Serious effort was devoted to the penetration shield as it significantly affects reactor cost, personnel access, and reactor operation. An elaborate three-dimensional (3D) radiation transport analysis for the complete reactor system, including the first wall, blanket, bulk shield, neutral beam injectors, divertor ducts, TF coils, and reactor building, were carried out. The general purpose Monte Carlo code MCNP was used for the calculations with a continuous energy representation for the nuclear cross sections based on ENDF/B-IV nuclear data files. The energy spectrum and spatial distribution of the neutron source from the D-T plasma were modeled in the calculations. Coupled neutron and neutron-induced photon transport calculations during operation, and decay photon transport calculations after shutdown were performed using the same geometrical model. The results show that a 100 cm outboard bulk shield thickness including a 4 cm thick layer of lead on the outermost surface of the shield behind a 50 cm tritium breeding blanket is needed to achieve the required dose equivalent level. A composition of 80% Fe-1422, 10% H_2O, and 10% B_4C by volume gives the best performance with the water and B_4C material located in the low neutron flux region. The 3D calculations show that the following shield thicknesses are required to satisfy the dose equivalant criterion: a) 105 cm for neutral beam drift tubes, b) 100 cm for the beam injector box surfaces facing the drift tubes, c) 75 cm for the top section of the injector boxes and the surfaces connected and perpendicular to the neutral beam drift tubes, d) 85 cm for the rest of the neutral beam systems, and e) 70 cm for the divertor ducts tapered to 30 cm at the outer end.

---

*Work supported by the U.S. Department of Energy.

INTRODUCTION

The U.S. INTOR radiation shield system was designed to perform several functions and satisfy the design constraints. The main function of the shield during reactor operation is to reduce the neutron and photon leakage intensities from the shield. This reduction ensures that a) the different reactor components are protected from radiation damage and excessive nuclear heating, b) the neutron reaction rates in the reactor components which produce undesirable radioactive isotopes are reduced, and c) the worker and the public are protected from radiation exposure. Another shield requirement is to attenuate the decay gamma rays so that personnel are permitted access to the reactor hall, with all shields in place within one day after shutdown. The personnel access to the reactor hall significantly reduces the reactor downtime and the capital cost of the remote equipment required for maintenance.[1]

The bulk shield analyses were performed in two steps to define the composition and material arrangement for the inboard and outboard portions of the reactor. First, extensive one-dimensional analyses were performed for a wide range of shield compositions using a homogeneous mixture model with Fe-1422 (a steel alloy with 14% Mn, 2% Ni, and 2% Cr), H_2O and B_4C materials. Next, the results from the homogeneous analyses were used for a heterogeneous analyses to account for the engineering details and neutronics benefits obtained by redistribution of the materials to improve the performance of the bulk shield.

Special effort was given to the dose equivalent in the reactor hall after shutdown and the penetration shield as they significantly affect reactor cost, personnel access, and reactor operation. An elaborate 3D radiation transport analysis for the complete reactor system, including the first wall, blanket, bulk shield, neutral beam injectors, divertor ducts, toroidal field coils, and reactor building, was carried out. The general purpose Monte Carlo code MCNP[2] was used for the calculations with a continuous energy representation for the nuclear cross sections based on ENDF/B-IV nuclear data files. The energy spectrum and spatial distribution of the neutron source from the D-T plasma were modeled in the calculations. Coupled neutron and neutron-induced photon transport calculations during operation and decay photon transport calculations after shutdown were performed using the same geometrical model to define the penetration shield thicknesses and the spatial distribution of the dose equivalent inside the reactor hall within one day after shutdown.

In this paper, the design criteria and constraints adopted for the INTOR design, the bulk shield optimization analyses and results are briefly presented. The geometrical model, neutron source, nuclear data, and calculational method used for the 3D analyses are described. The results during operation and one day after shutdown from the 3D calculations are discussed.

DESIGN CRITERIA AND CONSTRAINTS

In the design of a shielding system, a careful definition of the design criteria is an essental step.[3,4] The toroidal field (TF) coils are designed to last the lifetime of the reactor without change in their performance. Therefore, the shielding system must protect the different components of the TF coils from radiation damage. In general, neutron irradiation of the superconductor materials tends to lower the critical current density (J_c) and the

critical temperature (T_c). For Nb_3Sn superconductor, it has been shown[5] that T_c starts to experience a significant decrease at a neutron fluence above 10^{18} n/cm^2. The copper resistivity is more sensitive to the neutron fluence, where a neutron fluence of 10^{18} n/cm^2 generates an induced resistivity of 7×10^{-8} $\Omega \cdot cm$. This increase in the resistivity can be annealed out by warming the TF coils. The most sensitive component in the TF coils is the insulator materials because the radiation damage in them is irreversible and limits the operating life of the TF coils. It was demonstrated[6] that epoxy insulator (Kapton) can withstand a radiation dose of 10^{10} rads at cryogenic temperature and retains adequate resistivity and mechanical strength. The nuclear energy deposition in the TF coils impacts the refrigeration power requirement since about 300 to 500 watts of electrical power are consumed to remove one watt from the TF coils at 4°K. This removal efficiency calls for minimizing the nuclear energy deposition in the TF coils. From the above discussion and the INTOR design specifications, design criteria were established for the maximum permissible neutron fluence and dose to the TF coils. In summary, the design calls for the following criteria for the TF coils:

1) a maximum nuclear heating of 5 kW in the TF coils,
2) a maximum tolerable dose of 10^{10} rads in the insulator materials at the end of the operating life (6 $MW \cdot y/m^2$),
3) a maximum neutron fluence of 10^{18} n/cm^2 ($E > 0.1$ MeV) in the Nb_3Sn superconductor material at the end of the operating life, and
4) a maximum induced resistivity of 5×10^{-8} $\Omega \cdot cm$ in the copper stabilizer at the end of operating life.

The personnel access to the reactor hall within one day from shutdown requires the satisfaction of regulations pertaining to occupational exposure. All the regulations[7] limit the occupational dose to 5 rem/y with a maximum of 3 rem/quarter. Occupational exposure based on working 8 h per day and 40 h per week is 2.5 mrem/h. The outboard shield was optimized to minimize exposure dose in the reactor hall within one day from shutdown.

INBOARD BLANKET AND SHIELD

The main goal of the inboard blanket and shield is to protect the TF coils from radiation damage and excessive nuclear heating. The inboard blanket does not produce tritium, it only protects the TF coils. An optimization analysis based on a one-dimensional cylindrical model was performed in two steps to define the optimum composition and arrangement of the shield materials. First, the calculations were performed for a wide range of compositions using a homogeneous mixture for the inboard blanket and shield. Table 1 lists the blanket and shield parameters used in the calculations. Next, the results from the homogeneous model were used as input for a heterogeneous analysis to account for the engineering considerations and benefits from redistribution of the shielding materials to get more protection for the TF coils.

A sample of the results is given in Figs. 1 and 2. Figure 1 shows the nuclear heating in the TF coils per cm of the inboard section which includes superconductor zone, case, and dewar. The maximum nuclear heating in the TF case is shown in Fig. 2. The nuclear heating results have a flat minimum in the range of 10 to 30% B_4C with 65 to 80% Fe-1422, all percentages are referring to volume fraction. The maximum neutron fluence in the superconductor has a flat minimum in the range of 70 to 80% Fe-1422 concentration. The minimum is $\sim 5 \times 10^{17}$ n/cm^2 which is less than the threshold for the radiation damage

Table 1. Blanket and Shield Parameters Used in the One-Dimensional Bulk Shield Analyses

Zone Description	Major Radius (cm) From	To	Composition Volume Percentage
TF case	190	200	100% type 316 SS
TF superconductor	200	270	37.7% type 316 SS, 24% Cu, 2.6% Nb_3Sn, 28.5% He, 7.2% epoxy
TF case	270	280	100% type 316 SS
Thermal insulators	280	290	1% epoxy, 99% vacuum
TF dewar	290	295	100% type 316 SS
Vacuum gap	295	299	
Blanket and shield	299	374	X% Fe-1422, Y% B_4C[a], (100-X-Y)% H_2O
First wall	374	375	50% type 316 SS, 50% H_2O
Armor	375	380	100% C
Scrape-off	380	410	
Plasma	410	650	
Scrape-off	650	660	
Armor	660	661	100% type 316 SS
First wall	661	662	50% type 316 SS, 50% H_2O
Neutron multiplier	662	669.5	100% Pb
Second wall	669.5	670.5	50% type 316 SS, 50% H_2O
Tritium breeder	670.5	710	10% type 316 SS, 10% H_2O, 45% Li_4SiO_4, 35% He
Shield	710	806	X% Fe-1422, Y% B_4C[a], (100-X-Y)% H_2O
	806	810	100% Pb

[a] An 0.9 density factor is used for B_4C material.

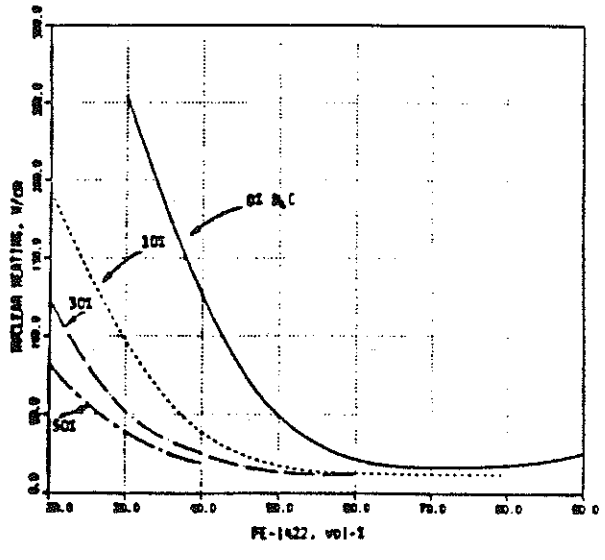

Fig. 1. Nuclear heating in the TF coils (superconductor case, and dewar) per cm of the inboard section normalized to 1.3 MW/m^2 neutron wall loading.

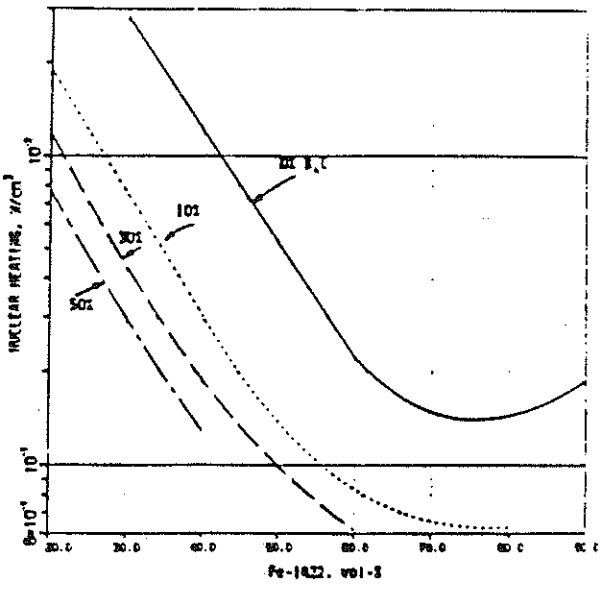

Fig. 2. Maximum nuclear heating in the TF case normalized to 1.3 MW/m^2 neutron wall loading.

in the Nb_3Sn superconductor. The dose insulator results show that the neutron dose accounts for more than 75% of the total dose for the blanket and shield with B_4C. The gamma dose in the insulator material is higher for lower B_4C concentrations because of the increase in the gamma flux caused by radiative capture of low energy neutrons in the Fe-1422 material. The maximum dose in the thermal insulator has a minimum value of 2.8×10^9 rads at 80% Fe-1422, 10% B_4C, and 10% H_2O composition after 6 MW·y/m^2 neutron exposure. From the above analyses, it appears that a composition of 80% Fe-1422, 10% B_4C, and 10% H_2O is an optimum choice for the magnet protection based on the homogeneous analysis.

The inboard blanket and shield design consists of two parts. The first part is integrated with the removable torus sector module and the second part is semi-permanent shield. The radial thickness of the first part is 20 cm. It consists of 5 cm carbon armor, 1 cm first wall, 12.5 cm bulk material, and 1.5 cm steel jacket for structure purpose. Type 316 stainless steel is used for the first part instead of Fe-1422. A 3 cm vacuum gap between the two parts is used to accommodate thermal expansion and engineering tolerance. The second part is divided into seven layers to define a possible heterogeneous arrangement which maximizes the magnet protection. Five layers of Fe-1422 with water coolant, each is 9 cm thick; and two layers of B_4C with steel cladding material and water coolant, each 5 cm thick, were considered. The equivalent homogeneous composition for both parts is the 80% steel, 10% B_4C, and 10% H_2O, as defined from the previous analysis. However, the total thickness of the materials included was reduced by 2 cm. Several arrangements were analyzed and compared to the homogeneous case. Table 2 gives the radiation response parameters in the inboard portion of the TF coils based on the best heterogeneous arrangement and the homogeneous case.

The heterogeneous results in Table 2 show that the maximum nuclear heating in the superconductor is reduced by 14% relative to the homogeneous case and the nuclear heating in the TF coils (superconductor and case) is almost the same. The nuclear heating in the dewar increases as compared to the homogeneous case due to the increase in the gamma heating. The gamma-ray flux is much higher in the heterogeneous arrangement because more low energy neutrons are absorbed through (n,γ) reactions in the Fe-1422. In the homogeneous shield, the boron carbide is uniformly distributed and reduces significantly the radioactive capture in the Fe-1422. The neutron fluence, copper-induced resistivity, insulator dose, and displacement per atom from the heterogeneous shield are reduced by 25% relative to the homogeneous case at 6 MW·y/m^2 neutron exposure. In fact, the neutron responses decrease while the gamma responses increase with a net decrease in the total responses. The reason for the increase in the gamma responses is due to the increase in the gamma rays production as explained before. The reduction in the neutron flux, which decreases the neutron responses, is caused by the use of more Fe-1422 in the front portion of the shield where iron is more effective in slowing down the high energy neutrons through inelastic scattering. Also, the use of more B_4C in the back portion of the shield causes softening and reduction for the neutron flux in the TF coils.

OUTBOARD SHIELD

In addition to radiation protection of reactor components, the design of the outboard shield is critical in satisfying the personnel access requirements. The dose equivalent in the reactor hall outside the bulk shield should

Table 2. Radiation Response Parameters in the Inboard Portion of the TF Coils Normalized to 1.3 MW/m^2 Neutron Wall Loading and 6 $MW \cdot y/m^2$ Neutron Exposure

Radiation Response Parameters	Homogeneous Analysis	Heterogeneous[a] Analysis
Maximum neutron fluence in the superconductor, E > 0.1 MeV (n/cm^2)	5.41×10^{17}	3.88×10^{17}
Maximum induced resistivity in the copper stabilizer (Ω-cm)	4.29×10^{-8}	3.14×10^{-8}
Maximum atomic displacement in the copper stabilizer (dPa)	3.39×10^{-4}	2.54×10^{-4}
Maximum nuclear heating in the superconductor (W/cm^3)	1.06×10^{-4}	9.16×10^{-5}
Nuclear heating in the superconductor and the TF case (W/cm)	7.22	7.21
Nuclear heating in the superconductor, TF case, and dewar (W/cm)	12.31	16.72
Maximum dose in the thermal insulator (rads)		
Neutron	2.09×10^9	1.6×10^9
Gamma	0.67×10^9	0.9×10^9
Total	2.76×10^9	2.5×10^9
Maximum dose in the electrical insulator (rads)		
Neutron	6.9×10^8	5.1×10^8
Gamma	1.9×10^8	1.7×10^8
Total	8.8×10^8	6.8×10^8

[a] The shield thickness in the heterogeneous analysis is 2 cm less than the homogeneous case.

be $\leq$ 2.5 mrem/h within one day after shutdown with all shields in place. Since decay gamma rays typically have a short mean free path in moderately heavy materials, the contribution to the dose equivalent comes essentially from the 5 to 15 cm of the materials facing inside the reactor hall. Therefore, satisfying the personnel access criterion requires that a) the bulk and penetration shields be effective in significantly reducing the neutron leakage; and b) materials in the outermost region of the shield do not produce strong decay gamma rays. Fe-1422, B_4C, and H_2O constitute a good material composition for the outer bulk shield. In addition, a small layer of lead in the outer region is beneficial as it attenuates the decay gamma rays from the inner region.

An optimization process was carried out to define a suitable composition similar to the inboard shield. A comprehensive analysis was performed to minimize the neutron energy leakage from the outboard shield. The neutron energy leakage was taken as a good measure of both the neutron flux intensity and the softening in the neutron spectrum. Softening the neutron spectrum is necessary to reduce the production rate of long-lived isotopes which are generated mainly by high energy reactions such as (n,2n) and (n,p). The calculations were performed with the same compositions used for the inboard shield analyses in the previous section with a 90-cm total shield thickness behind the 50 cm tritium

breeding blanket. For average neutron energy leakage of less than one MeV, the analysis shows that the minimum neutron leakage occurs with a composition of 80% Fe-1422, 10% B_4C, and 10% H_2O ($\sim 2 \times 10^{-7}$ neutron per fusion neutron) based on the homogeneous calculations.

In the heterogeneous analysis for the outboard shield, the shield thicknesses is divided into eleven different layers: eight layers are 9 cm thick each and three layers are 5 cm thick each, and two steel jackets are 1.5 cm thick each. Each of the 9 cm layers has Fe-1422 mixture (90% Fe-1422, 10% H_2O by volume) and each of the 5 cm layers has B_4C mixture (40% B_4C, 20% Fe-1422, 40% H_2O by volume). The average composition of the materials is equivalent to the homogeneous one defined before. The best material arrangement reduces the neutron energy leakage by a factor of two relative to the homogeneous case. The neutron flux from the heterogeneous arrangements show a significant decrease except in the 3-8 MeV energy range where a very small increase occurs.

The dose equivalent calculations after shutdown were performed for several heterogeneous arrangements as a function of the shield thickness. A sample of the results is given in Table 3 for two cases. The first case represents the optimum configuration to reduce the dose equivalent within one day after shutdown. The maximum dose equivalent occurs near the magnet dewar of the TF coils. The second shield in Table 3 uses more water and less Fe-1422 compared to the optimum shield.

Table 3. Shield Specification and Dose Equivalent One Day After Shutdown

Parameter	Shield Option 1		Shield Option 2	
Total shield thickness	100 cm		105 cm	
Shield specification				
Shield jacket	1.5 cm	100% Fe-1422	1.5 cm	100% Fe-1422
Steel shield	85 cm	90% Fe-1422, 10% H_2O	68 cm	90% Fe-1422, 10% H_2O
Boron shield	8 cm	56% B_4C, 10% H_2O, 10% Fe-1422	30 cm	36% B_4C, 40% H_2O, 20% Fe-1422
Shield jacket	1.5 cm	100% Fe-1422	1.5 cm	100% Fe-1422
Lead shield	4 cm	100% Pb	4 cm	100% Pb
Dose equivalent one day after shutdown, mrem/hr				
End of the shield		0.56		0.35
Magnet dewar surface		1.06		0.61
Dose equivalent one week after shutdown, mrem/hr				
End of the shield		0.25		0.17
Magnet dewar surface		0.72		0.55

THREE-DIMENSIONAL SHIELDING ANALYSES

In order to define the dose equivalent in the reactor hall and the penetration shield thicknesses, elaborate calculations were carried out in great detail. A 3D model describing the details of the reactor system was used in the analysis. The geometrical model, neutron source, nuclear data, calculational method, and the results from the 3D analyses are discussed briefly.

Geometrical Model

The 3D geometrical model shown in Fig. 3 describes the whole reactor where the different reactor components are presented explicitly. The model makes use of the reactor symmetry (12 toroidal field coils, 6 neutral beam injectors, 6 divertor ducts) by considering a 30° sector. This sector includes one TF coil, one-half divertor duct, and one half NB injector as shown in Fig. 3. The inner portion of the TF coil is represented by a set of concentric cylinder surfaces where the radii and the zone compositions are listed in table 1. The outer portion of the TF coil is represented by a set of ellipsoid surfaces intersected by a set of vertical planes. The TF case and dewar thickness are 10 cm each. The thermal insulator zone thickness is 10 and 15 cm for the inner and outer portions of the TF coil, respectively. The superconductor is 70 cm in the radial direction for both portions of the TF coil and 100 cm in the toroidal direction for the outer portion. The NB injector port size and divertor duct dimension are 1.2 x 1.0 and 1.3 x 0.5 m in the vertical and toroidal direction, respectively. The building liner is represented by a 10 cm layer of type 316 stainless steel.

Neutron Source

The neutron source distribution function [$s(r,z) \cdot n(E)$] was used for the analyses. Where $s(r,z)$ represents the spatial distribution and $n(E)$ gives the energy spectrum. The spatial distribution is based on the fusion power density and defined as follows:

$$s(r,z) \alpha [1 - (r/r_m)^2]^2 , \qquad (1)$$

where r is the distance measured from the plasma center to the source point defined by (r,z), r_m is the distance measured from the plasma center to the plasma boundary passing through the same source period. The plasma boundary is fitted to a D-shape as follows:

$$Z = a_o \, k \sin t,$$
$$\rho = R_o + a_o \cos (t + 0.27 \sin t) . \qquad (2)$$

where (ρ,Z) describes a point on the plasma boundary; t is a parameter which varies from 0 to 180°, a_o is the plasma radius 120 cm, k is the plasma elongation 1.6, and R_o is the plasma major radius 545 cm.

The energy spectrum of 14 MeV-neutron from the DT plasma is described by a Gaussian distribution as follows:

$$n(E) \alpha \exp \left[- \left(\frac{E-b}{a}\right)^2\right] \qquad (3)$$

where b = 14.057 MeV and a = 0.3359 MeV.

Nuclear Data and Method of Calculations

Continuous energy representation for the nuclear cross sections (pointwise data) was used for the transport calculation. All the nuclear cross sections were generated from ENDF/B-IV data files except for manganese and molybdenum. The nuclear cross sections for these two elements were generated from ENDL data files. The neutron and photon energy ranges were 2.2×10^{-8} to 15 MeV and 0.01 to 15 MeV, respectively, for the calculation.

The neutron and neutron-induced photon transport calculations were performed with the MCNP code. Three variance reduction schemes were employed for the calculations. These are splitting, Russian roulette, and weight cutoff with Russian roulette. Neutron fluxes and nuclear heating rates were calculated in all zones. In addition, nuclear heating rates averaged over segmented zones were calculated for the different reactor components.

In order to calculate the dose equivalent in the reactor hall, a 3D dose analysis was performed. The neutron fluxes from the 3D neutron transport calculation were used to generate a decay gamma source (via DKR code) at 24 h after shutdown in every reactor zone. Using this source and the same geometrical model, a gamma transport calculation was carried out to obtain the gamma fluxes, gamma heating, and radiation exposure dose in several locations in the reactor hall. Several iterations were performed to define the penetration shield thicknesses for the divertor and NB systems. Each iteration repeats the whole calculational procedure.

Results and Analysis

A coupled neutron and neutron-induced photon transport calculation was performed with 10^5 D-T neutrons where a sufficient statistical accuracy was obtained in the different reactor components. The results show that a nuclear heat deposition of about 3.6 kw in the TF coils (TF case and superconductor) is obtained; the design specification sets a maximum of 5 kw. Figure 4 shows the nuclear heating in the surface of the neutral beam drift tube and the neutral

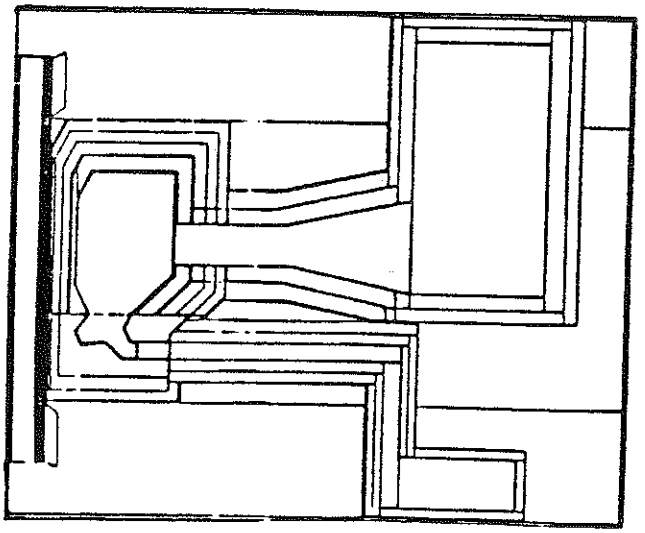

Fig. 3. Vertical cross-section of the 3D geometrical model.

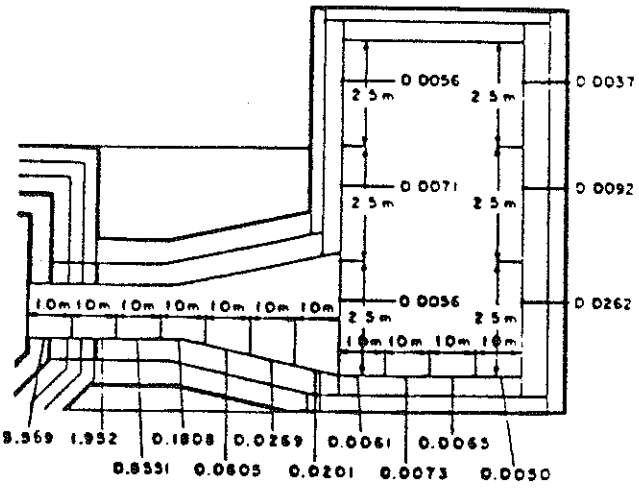

Fig. 4. Surface nuclear heating in the neutral beam injector (W/cm^3).

beam injector box, averaged for different segments of the surface during the burn cycle, with the shutter open. The nuclear heating in the drift tube is averaged for 100 cm segments starting from the first wall. The surface of the neutral beam box is divided into three parts: the first part faces the neutral beam drift tube and is perpendicular to the neutral beam drift tube axis; the second part is parallel to the first part but does not directly face the plasma; and the third part is the rest of the neutral beam box which consists of three surfaces parallel to the neutral beam drift tube. The maximum nuclear heating occurs in the area facing the plasma, as shown in Fig. 4. The maximum nuclear heating in the vacuum pumps located in the neutral beam boxes without a direct sight to the plasma is ~ 3 kW at full neutron power with the shutter open. The nuclear heating in the vacuum pumps of the divertor is less than 1 W due to the long L-shape duct (~ 1400 cm).

The maximum dose equivalent calculated from the decay gamma transport is 2.81 mrem/h with 0.24 fractional standard deviation between the TF coils. In order to achieve this dose equivalent, the following shield thicknesses are required based on several iterations: a) 105 cm for neutral beam drift tubes, b) 100 cm for the beam injector box surfaces facing the drift tubes, c) 75 cm for the top section of the injector boxes and the surfaces connected and perpendicular to the neutral beam drift tubes, d) 85 cm for the rest of the neutral beam systems, and e) 70 cm for the divertor ducts tapered to 30 cm at the outer end. The shield composition in the 3D analyses is the second option shown in table 3.

REFERENCES

1. W. M. Stacey, et al., "U.S. INTOR, The U.S. Contribution to the International Tokamak Workshop," (November, 1979).

2. LASL Group X-6, "MCNP - A General Monte Carlo Code for Neutron and Photon Transport, Version 2B," Los Alamos National Laboratory, LA-7396-M, Revised (April, 1981).

3. Y. Gohar, "Low Cost Shield for Tokamak Fusion Reactors," 5th Topical Meeting on the Technology of Fusion Energy, Knoxville, Tennessee, (April 26-28, 1983).

4. M. A. Abdou, "Radiation Considerations for Superconducting Fusion Magnets," J. Nucl. Mater. 72 (1&2), 147 (1978).

5. B. S. Brown, "Radiation Effects in Superconductor Fusion-Magnet Materials," J. Nucl. Mater. 97 (1&2), 1 (1981).

6. R. R. Coltman, et al., "Effect of Radiation at 5°K on Organic Insulators for Superconducting Magnets," Proc. 8th Symp. on Engineering Problems of Fusion Research, Vol. III, p. 1694 (1979).

7. U.S. Nuclear Regulatory Commission, Standard for Protection Against Radiation," USNRC Rules and Regulations, Title 10, Chapter 1, Part 20 (1977).

Paper presented at the 6th International Conference on Radiation Shielding (6th ICRS), May 16-20, 1983, Tokyo, Japan. To be published in proceedings of the conference.

U.S. INTOR RADIATION SHIELD DESIGN*

Y. Gohar and M. A. Abdou **

Fusion Power Program
Argonne National Laboratory
9700 South Cass Avenue
Argonne, IL 60439

May, 1983

* Work supported by the U.S. Department of Energy.
** Now located at University of California, Los Angeles.